Hindawi Publishing Corporation
ISRN Polymer Science
Volume 2013, Article ID 284504, 9 pages
http://dx.doi.org/10.1155/2013/284504

Research Article

Effect of Filler Dimensionality on Mechanical Properties of Nanofiller Reinforced Polyolefin Elastomers

Sharmila Pradhan,[1,2] Ralf Lach,[3,4] Hong Hai Le,[3] Wolfgang Grellmann,[3,4] Hans-Joachim Radusch,[3] and Rameshwar Adhikari[1,2]

[1] *Central Department of Chemistry, Tribhuvan University, Kirtipur, Kathmandu, Nepal*
[2] *Nepal Polymer Institute (NPI), P.O. Box 24411, Kathmandu, Nepal*
[3] *Centre of Engineering, Martin-Luther University Halle-Wittenberg, 06099 Halle/Saale, Germany*
[4] *Institute of Polymer Materials, Institute Associated with the University of Applied Science Merseburg, Geusaer Straße Geb. 131, 06217 Merseburg, Germany*

Correspondence should be addressed to Ralf Lach; ralf.lach@psm.uni-halle.de and Rameshwar Adhikari; nepalpolymer@yahoo.com

Received 10 April 2013; Accepted 19 May 2013

Academic Editors: C.-Y. Guo, B. Hazer, and C. Liu

The object of this study has been to investigate the effect of filler dimensionality on morphology and mechanical properties of polymer nanocomposites using various kinds of nanofillers (such as multiwalled carbon nanotubes (1D filler), layered silicate (2D filler), and boehmite (3D filler)) dispersed in the matrix of ethylene-1-octene copolymer (EOC), a polyolefin-based elastomer. The morphological features were studied by scanning electron microscopy (SEM) and differential scanning calorimetry (DSC) while mechanical properties were characterized by tensile testing and depth sensitive recording microindentation hardness measurements. It has been demonstrated that the filler dimensionality may have dramatic influence on the mechanical properties of the samples. Based on the results obtained by tensile testing and microhardness measurements, the reinforcing effect of the nanofiller was found to follow the order: 1D filler > 2D filler > 3D filler.

1. Introduction

The development of multifunctional engineering materials possessing novel properties has been achieved with the addition of nanosized filler which has overcome several disadvantages of traditional composites. Thus, such novel polymeric materials incorporated with fillers having ultrafine phase dimensions typically of less than 100 nm, which are especially termed as polymer nanocomposites (PNCs), have attracted special research interest [1–9]. Through the variation in particulate dimension from micrometer to nanometer scale, the surface area to volume ratio has been found to alter by three orders of magnitude leading to the drastic changes in morphological features as well as in their properties in such materials [3–9].

The new polymer nanocomposites have been fabricated generally with three categories of reinforcing materials such as particles (e.g., silica, metal, and other organic and inorganic substances), layered materials (e.g., graphite, layered silicate, etc.), and fibrous materials (e.g., nanofibers and nanotubes) [4–10]. Compared to conventional counterparts, these nanocomposites have been found to possess promising mechanical properties such as hardness, tensile modulus, strength, and toughness at both low and high temperatures. In addition, the PNCs are found to have significantly improved barrier properties, thermal stability, and extinguishing characteristics with advantage of light weight of the common polymers [1]. Thus, these are used as excellent prospective materials for food packaging, membranes, adhesives, automotive parts, textiles, and so forth. [11].

Furthermore, the material properties distinctly depend not only on the size of the reinforcement particles but also on the properties of the interphase. A thorough review of the literature reveals the role of intercalated and interphase

volume on the physical properties of the PNCs [12, 13]. In case of the presence of weak particle/matrix interface, the mode of plastic deformation in glassy polymers changes from cavitation to shear yielding leading to a transition from brittle to ductile behavior [14]. The change in deformation behavior has been attributed to the increased polymer chain mobility, presence of smaller particles, and also the capability to relieve triaxial stress because of poorly bonded larger particles [3]. The large surface area of the nanofillers results in large volume fraction of interfacial matrix material with properties entirely different from the bulk polymer. The interfacial area creates significant volume fraction of interfacial polymer even at low loadings (<5 vol. %). The thermal, mechanical, and electrical properties of the composites have also been affected directly with interfacial polymer [15]. In addition, it has been pointed out that the structure and properties of interfacial polymer are the controlling factor for changes in crystallinity, mobility, chain conformation, chain entanglement, density, and charge distribution of thermoplastic polymer-based PNCs [16].

Mechanical properties of polymeric materials are largely determined by their molecular structure, morphology, and processing methods [17]. In particular, the microhardness can be determined by variety of instruments differing in the shape of indenters (such as Rockwell, Brinell, Vickers, and Knoop). Among various methods of measuring the microhardness, the recording indentation technique offers the most promising and simplest way as this method has several advantages such as less time consuming, small volume of the sample, and no need of preparing the special specimen [15–23]. It has been shown recently that the microhardness of glassy polymers (such as polycarbonate, PC) based composites is dependent on the structure and dimension of the nanoparticles used [24]. The filler particles having considerable length of any of the dimensions relative to the rest of the others are said to be one-dimensional (or 1D) fillers. If two or three of such dimensions are of considerable lengths, then the fillers are said to be two dimensional (2D) or three dimensional (3D), respectively. More recently, it has been demonstrated that various kinds of polymer nanocomposites alter mechanical properties drastically with the dimensionality of fillers (1D, 2D, and 3D) [25].

In this line, the uniaxial-tensile (secant modulus at 10% strain) and hardness properties (Shore-A hardness) of ethylene-1-octene copolymer (EOC) elastomers containing multiwalled carbon nanotubes (MWCNT) and expandable graphite were investigated recently [26, 27]. However, a direct correlation between the filler dimensionality and mechanical properties of PNCs has not been well explained in the literature yet. The objective of this work is to analyze the structure-property correlation in PNCs formed by 1D, 2D and 3D fillers using the commercially available ethylene-1-octene copolymer elastomer as matrix polymer.

2. Experimental Section

2.1. Materials and Sample Preparation. Ethylene-1-octene copolymer (EOC), a commercial product of Dow Chemical Company (trade name: Affinity EG8150) having molecular weight of 161,400 g/moL, and melt flow index (MFI) of 0.5 g/min were used as the polymer matrix. The degree of crystallinity of the EOC is 16% and comonomer content is 39%.

Various types of nanofillers like multiwalled carbon nanotubes (named MWCNT in this work) manufactured by Bayer Materials (commercial name: Baytubes), organically modified layered silicate (named LS in this work) developed by Südchemie (commercial name: Nanofil 5), and boehmite nanoparticles manufactured by Sasol Chemicals (named OS2 in this work) representing 1D, 2D, and 3D fillers, respectively, were used. The MWCNT used was used without any surface chemical modification. The layered silicate filler is a organophilic modified montmorillonite with layer thickness of 1 nm in which distearyl dimethyl ammonium chloride has been used as organophilic modifier. The boehmite nanofiller (commercial name: Disperal OS2, Sasol) has an alumina hydrate (Al(OH)O structure coated with C10–C13 alkylbenzene sulphonic acid.

EOC nanocomposites containing 2 and 5 wt% of various nanofillers were prepared by melt mixing followed by compression molding. Melt mixing was carried out in an internal mixture maintained at 90°C and torque of 50 rpm for 10 minutes. Then the mixture was compressed to the sheets of 1 mm thickness at a temperature of 120°C and pressure of 110 bar. Tensile specimens (type 5A according to ISO 527) with length of 75 mm were punched out of the sheets.

2.2. Characterization Techniques

2.2.1. Scanning Electron Microscopy (SEM). The morphology of the nanocomposites was characterized by scanning electron microscope (SEM) JSM 6300 (JOEL) by using back scattered electron (BSE) imaging mode. Each specimen was cryofractured and sputter-coated with approximately 10 nm thick layer of carbon film prior to SEM imaging. The contrast in the BSE images directly correlates with the difference in the atomic mass of the elements present and hence represents the materials contrast [28].

2.2.2. Differential Scanning Calorimetry (DSC). The DSC measurements were performed on Mettler Toledo Differential Scanning Calorimeter (DSC 820) within a temperature range of −80°C to 150°C at a heating/cooling rate of 20 K/min.

2.2.3. Tensile Testing. The tensile stress-strain curves of each nanocomposite of EOC were recorded using dog bone shaped specimen by Zwick Z020 universal tensile tester (Zwick/Roell Co., Germany). The measurement was carried out at 23°C, at the cross-head speed of 50 mm/min.

2.2.4. Microindentation Test. The indentation measurements were carried out with the aid of a Fischerscope H100C recording microhardness tester equipped with a pyramidal Vickers diamond indenter (Helmut Fischer Co., Germany). The indenter was penetrated into the sample applying the force up to 300 mN at 23°C, the loading rate for both loading and unloading cycles being 15 mN/s. The evaluation of load

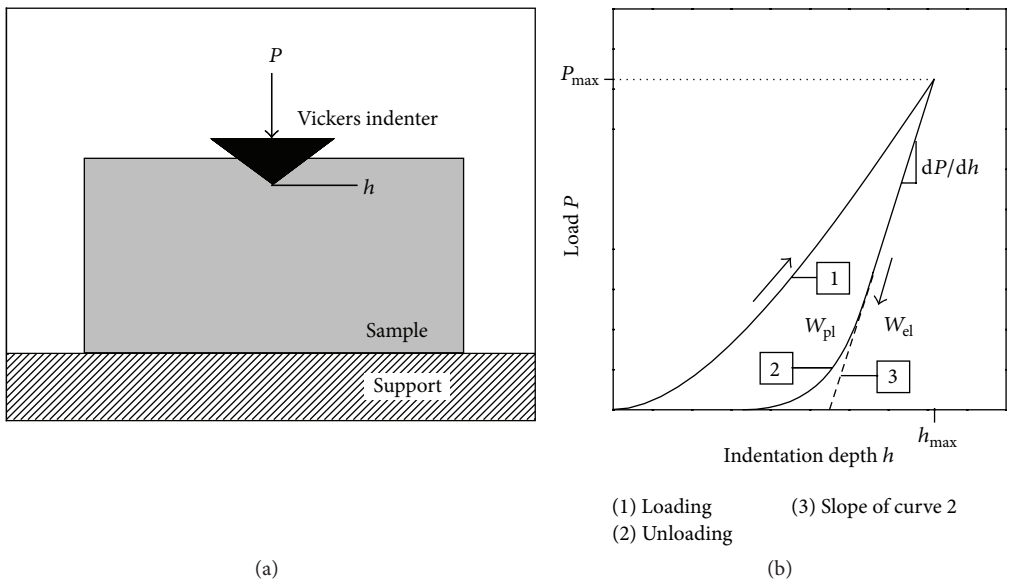

Figure 1: Scheme showing principle of indentation measurements (a) and typical loading-unloading curve obtained from an instrumented indentation (b); W_{el} and W_{pl}-elastic and plastic work of deformation, P_{max} and h_{max} maximum force and indentation depth.

(P) versus indentation depth (h) curves permitted the determination of both plastic (W_{pl}) and elastic (W_{el}) works of deformation, different hardness parameters (such as Martens hardness), and indentation modulus [24, 29].

The Martens hardness (HM) of each sample was determined using the following relation (ISO 14577-1 [30]):

$$\mathrm{HM} = \frac{P(h)}{A_s(h)} = \frac{P(h)}{26.43 \cdot h^2}, \tag{1}$$

where $A_s(h)$ is the surface area of the indenter penetrating beyond the zero point of the contact (with P in mN, h in μm, and HM in MPa).

The indentation depth is recorded with correction for small values of the indentation depth ($h < 6\,\mu$m) due to the erroneous indenter-tip configuration and the stress concentration for the material below the tip. To eliminate the influence of the specimen surface affecting the bulk hardness such as due to the surface roughness, we favour here the so-called Vickers hardness under load (L_2VH) over the Martens hardness (HM). L_2VH was calculated from the slope of the $P(h)/h$ versus h plots (for more information see Lach et al. [29]) as

$$L_2\mathrm{VH} = \frac{1}{26.43} \cdot \frac{\mathrm{d}\left(P(h)/h\right)}{\mathrm{d}h}. \tag{2}$$

Furthermore, besides the work done due to elastic and plastic deformation (W_{el} and W_{pl}, resp.), the indentation modulus (E_{IT}) was measured by applying (3) according to ISO 14577-1 [29, 30]

$$E_{IT} = \frac{1-\nu^2}{0.5 \cdot \sqrt{24.5/\pi} \cdot (\mathrm{d}h/\mathrm{d}P) \cdot \left(4h_{max} - 3P_{max} \cdot (\mathrm{d}h/\mathrm{d}P)\right) - 8.73 \times 10^{-13}\,\mathrm{Pa}^{-1}}. \tag{3}$$

Here, $\mathrm{d}h/\mathrm{d}P$ is the compliance of the contact, that is, the reciprocal slope of the initial unloading curve; P_{max} and h_{max} are the maximum force and indentation depth; ν is the Poisson's ratio of the material (ν is close to 0.33–0.38 for most thermoplastics polymers). The term $8.73 \times 10^{-13}\,\mathrm{Pa}^{-1}$ in (3) is the effective compliance of diamond used as the indenter. All data are averages of five measurements done on different positions on the films having a thickness of about 1 mm.

The obtained data were analyzed to understand the effect of filler weight fraction and its dimensionalities on the mechanical properties of polymer nanocomposites. Figure 1(a) shows the schematic diagram for the indentation test and Figure 1(b) shows the representative loading-unloading curves obtained from an instrumented indentation test. The Vickers hardness under load (L_2VH) was determined using (2) for $h \geq 6$–$9\,\mu$m. The indentation modulus E_{IT} can be obtained from the slope of the initial part of the unloading curve close to P_{max}. Furthermore, the elastic and plastic work of deformation, W_{el} and W_{pl}, and the total work of deformation $W_t = W_{el} + W_{pl}$ can be be determined from the P-h diagrams (Figure 1(b)).

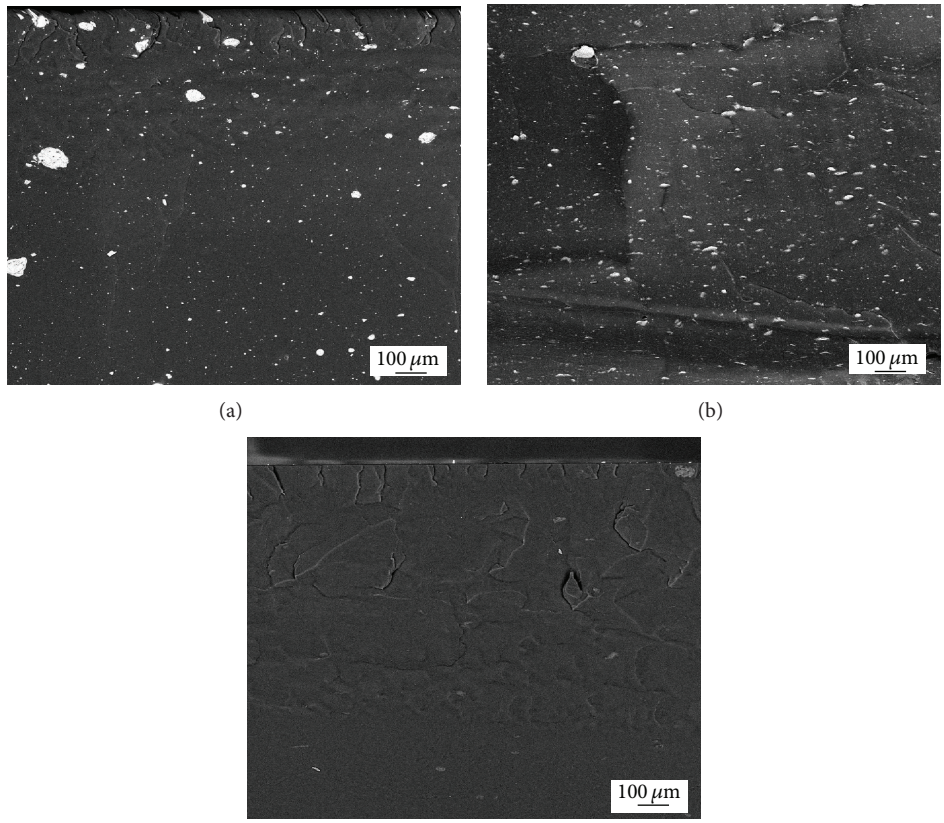

(a) (b)

(c)

Figure 2: BSE mode SEM micrographs of the nanocomposites comprising 5 wt% of different nanofiller: (a) boehmite (OS2, 3D filler), (b) layered silicate (LS, 2D filler), and (c) multiwalled carbon nanotubes (MWCNT, 1D filler).

3. Results and Discussion

3.1. Morphological Characterization of PNCs. Using BSE mode imaging, scanning electron microscopy (SEM) was used to inspect the dispersion of the nanoparticles in the polymer matrix (Figure 2).

Figure 2(a) shows the back scattered electron imaging of the nanocomposites comprising 5 wt% of OS2, the 3D filler. The SEM image of the sample shows clear dispersion of OS2 nanoparticles in the form of white dots. The largest boehmite particles of several micrometers in diameter due to agglomeration are distinctly visible. The SEM images presented in Figure 2 show the uniform distribution of the fillers with wide variation of particle diameter. The particles with nanometer dimension can be, however, invisible due to limited resolution of the SEM.

Figure 2(b) shows the fracture surface morphology of the PNC containing 5 wt% LS, the 2D filler. The SEM imaging shows well-dispersed LS particles in the form of fine white dots. Here, the particle diameter is narrower than the PNC with the boehmite nanoparticles indicating better compatibility of LS with the polymer. Figures 2(a) and 2(b) show clearly the agglomeration of the nanoparticles. Nevertheless, the aggregates show reasonably good distribution.

The SEM micrograph of EOC consisting of 5 wt% MWCNT (the 1D filler) depicted in Figure 2(c) shows the dark surface of the polymer, in which the nanoparticles could not be observed indicating that MWCNT and polymer have no mass contract between the inorganic filler and carbon present in the polymer. Nevertheless, no agglomerates are visible implying the good dispersion of the nanofiller.

The melting and crystallization behavior of the nanocomposites comprising 5 wt% of nanofiller each is compared with that of pure EOC in Figure 3. At the first glance, it can be observed that the main melting peaks of EOC and the nanocomposites occur at about 46°C while the nanocomposite with MWCNT melts at slightly lower temperature. In addition, for each sample, a shoulder appears at higher temperature region of the melting curve (see Figure 3(a)) at about 61°C. The melting endotherms are quite similar under given experimental conditions. The existence of two independent melting peaks signifies the presence of the two different kinds of crystalline entities in the samples. However, as the second peak was found to disappear on performing the second heating cycle on the sample, the second peak can be mainly correlated with the processing history of the samples.

The crystallization behavior of the nanocomposites is compared with that of pure EOC in Figure 3(b). As in the case of melting behavior, the samples show the crystallization peak centered around 41°C which is again a few degrees lower for the nanocomposites filled with 1D nanofiller, that is, multiwalled carbon nanotubes (MWCNTs). A secondary

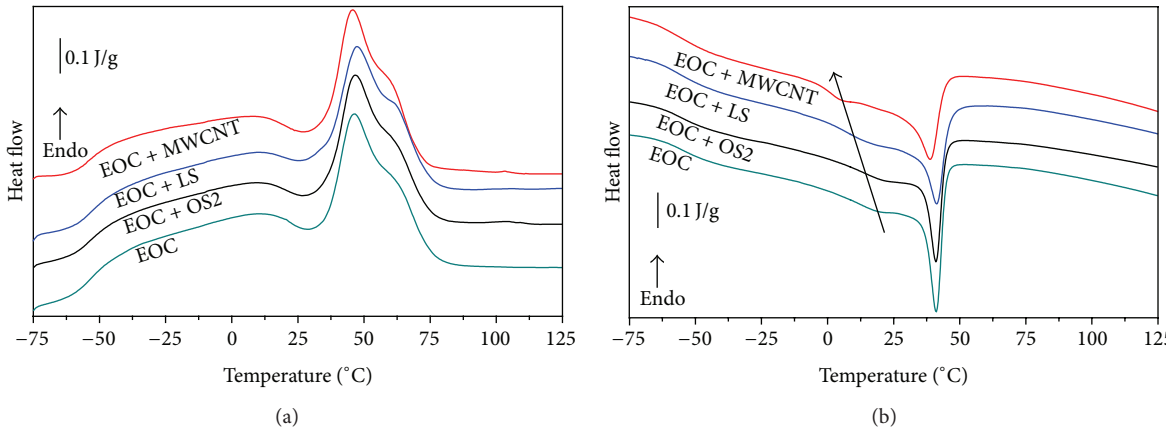

Figure 3: DSC plots showing heating (a) and cooling (b) runs of the nanocomposites compared with those of pure EOC matrix; the filler content in each composite is 5 wt%; heating and cooling rate is 20 K/min.

crystallization peak occurs around 19°C in the EOC as well as in the nanocomposites which, however, becomes broader compared to that of the pure EOC. A closer look in the endotherms presented in Figure 3(b) suggests that the broadening effect becomes pronounced with the decrease in dimensionality of the filler, shifting the crystallization peak towards lower temperature. In case of 1D filler containing nanocomposite, even a distinct new peak appears at much lower temperature (i.e., around 6°C). The results so far obtained indicate that there is different influence of the investigated fillers on the crystallization kinetics of the nanocomposites which needs further investigations. The fact that the morphological features of the composite comprising 1D nanofiller (i.e., MWCNT) show more significant shift also hints on larger influence of the MWCNT on mechanical and micromechanical behavior of the composites.

3.2. Tensile Properties of PNCs. Figure 4 compares the stress-strain curves of nanocomposites with the ethylene-1-octene copolymer. For each case, each curve is an average of 6 different measurements. Figure 4(a) compares the stress-strain curves of nanocomposites having different weight fraction of boehmite with pristine EOC. The curves of all the samples in this case are almost identical indicating that the boehmite, the 3D filler, could not reinforce the tensile property though it is well dispersed in the matrix (see Figure 2(a)). It seems that the boehmite could not make the chemical linkages with EOC and/or exhibits only little physical interplay with the macromolecules.

The stress-strain curves of virgin polymer and EOC filled with different weight fraction of layered silicate are presented in Figure 4(b). The curves presented are not much different; however, tensile strength is found to be increased slightly with the filler content. Thus the reinforcing effect of 2D filler is better than that of 3D filler. The influence of the dimensionality (1D, 2D, and 3D), that is, the aspect ratio, of the nanofiller is much more pronounced concerning the tensile modulus (Figure 5). The tensile modulus has been found to be larger for EOC/MWCNT (1D filler) than for EOC/LS (2D filler) and EOC/OS2 (3D filler) for both filler weight fractions (2 and 5 wt%) investigated. The value of the tensile modulus of pure EOC increases by more than 85%, 31%, and 14% through the incorporation of 5 wt% MWCNT, LS, and OS2 filler, respectively. For comparison, Osazuwa et al. [26] found recently an increase in tensile modulus of 54%–69% incorporating 3 wt% MWCNT into EOC.

The modulus of EOC/boehmite nanocomposites can be estimated theoretically by $E = E_0 \cdot e^{2.5\phi}$, where E, E_0, and ϕ are the tensile modulus of the nanocomposites and pure EOC and the volume fraction of 3D nanoparticles, respectively (for calculation of the particle's volume fractions, the density of EOC (0.868 gcm^{-3}) and boehmite (3.03 gcm^{-3}) were used) [31]. Interestingly, the estimated values do not match the experimentally determined ones probably since the nanoparticles affect the surrounding matrix polymer to a high degree resulting in regions of interfacial material having different properties [32].

The tensile curves of composites containing different weight fractions of MWCNT (see Figure 4(c)) show the decreasing trend of strain at break with filler content but the decrease is not significant. However, it is evident from Figure 4(c) that the stress at every strain is found to be increased with the amount of particles in the nanocomposites implying that the MWCNT, the 1D filler, is the most effective in reinforcing tensile property of the nanocomposites among the three different types of fillers.

3.3. Indentation Microhardness Measurement of PNCs. The microhardness and the elastic properties were determined by recording microindentation measurements [29].

The averaged load (P) versus corrected indentation depth (h) diagrams of pure EOC and EOC/OS2 nanocomposites is presented in Figure 6(a) which shows the identical curve patterns independent of the amount of boehmite (i.e., OS2) nanofiller present. However, the initial slope of the unloading curves of EOC/OS2 composites having varied weight fractions of OS2 appears lesser than that of virgin EOC curve. Hence, further addition of boehmite results in negative impact in the microindentation hardness of the polymer.

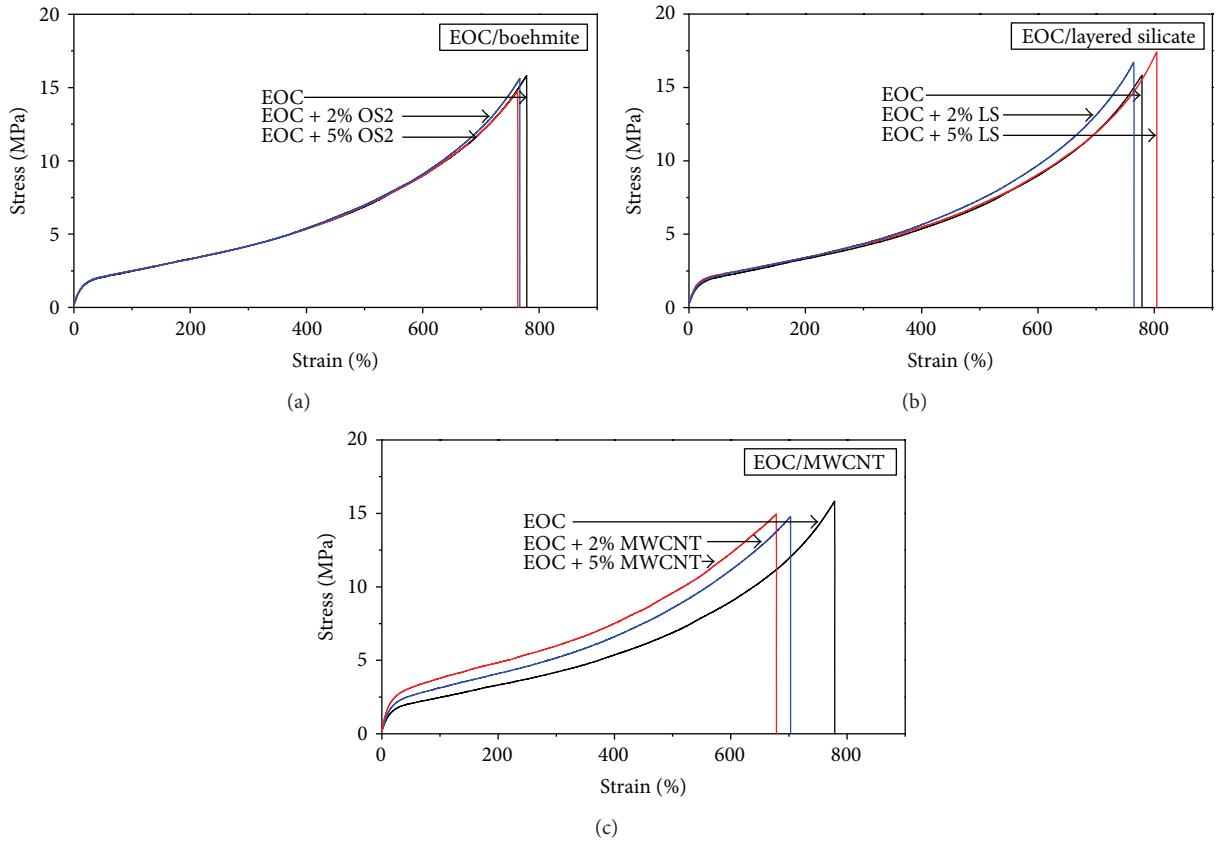

Figure 4: Stress-strain curves of PNCs consisting of varied weight fraction of different fillers: (a) PNCs comprising boehmite (3D filler), (b) PNCs with LS (2D filler), and (c) PNCs with MWCNT (1D filler).

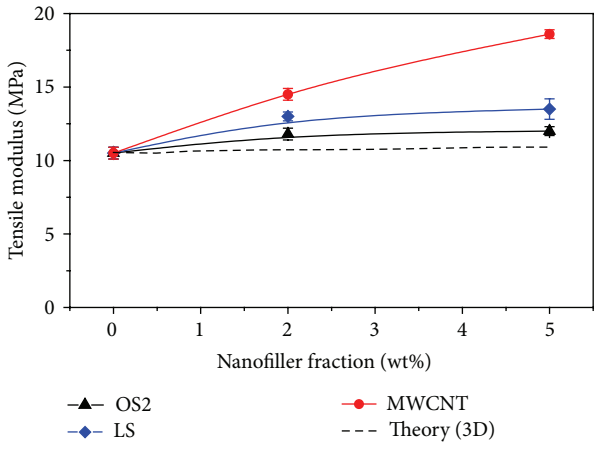

Figure 5: Tensile modulus of nanocomposites (EOC/OS2, EOC/LS, and EOC/MWCNT) as a function of nanofiller weight fraction.

The *P-h* curves of the EOC/layered silicate nanocomposites are presented in Figure 6(b). The experiments were carried out under identical conditions as in the sample presented in Figure 6(a). A closer view of plots of pure EOC and EOC modified with varied amount of LS reveals slight increment in the microhardness behavior of LS filled EOC samples.

Table 1: Mechanical properties (including the standard deviations) of the nanocomposites determined by microindentation test.

Nanofiller	Content (wt%)	L_2VH (MPa)	$E_{IT}/(1-\nu^2)$ (MPa)
None	—	0.865 ± 0.004	17.71 ± 0.31
OS2	2	0.771 ± 0.003	16.68 ± 0.89
	5	0.764 ± 0.003	18.76 ± 0.43
LS	2	0.886 ± 0.004	19.28 ± 0.40
	5	0.976 ± 0.004	21.87 ± 0.68
MWCNT	2	1.131 ± 0.005	20.27 ± 1.37
	5	1.387 ± 0.006	21.23 ± 0.55

In a similar manner, Figure 6(c) represents mean *P-h* curves of pristine EOC and EOC/MWCNT nanocomposites comprising multiwalled carbon nanotubes (MWCNT) of different weight fractions. Figure 6(c) clearly shows that the initial slope of the EOC/MWCNT comprising 5 wt% nanocomposites is higher than that of EOC/MWCNT containing 2 wt% and pure EOC sample. Hence, the addition of varied fractions of MWCNT reinforces the matrix polymer (i.e., EOC) significantly. The values of Vickers hardness under load (L_2VH) and indentation modulus (i.e., $E_{IT}/(1-\nu^2)$) obtained from the evaluation of the *P-h* diagrams presented in Figure 6 are indexed in Table 1 and plotted in Figure 7.

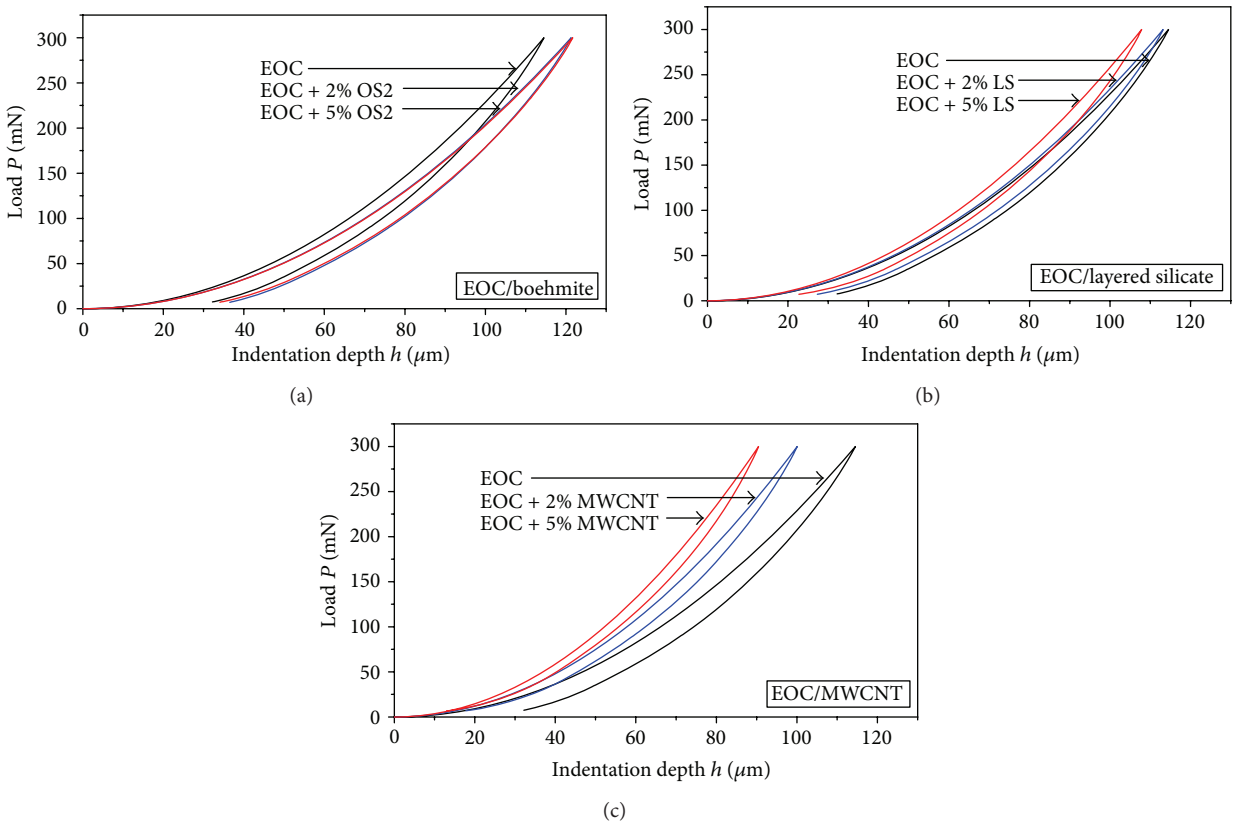

Figure 6: P-h diagrams of nanocomposites as a function of nanofiller weight fraction: (a) EOC/OS2, (b) EOC/LS, and (c) EOC/MWCNT.

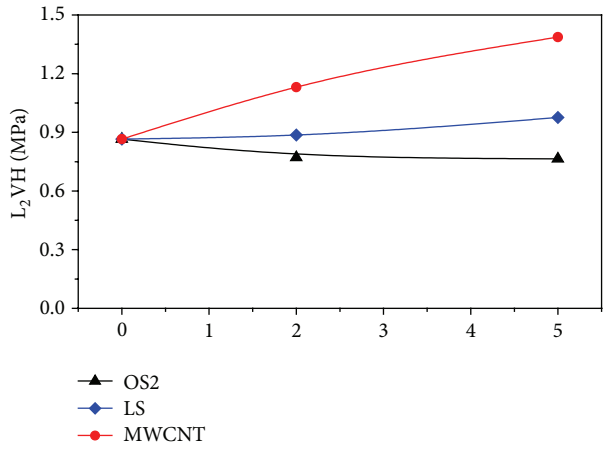

Figure 7: Vickers hardness under load (L_2VH) of nanocomposites (EOC/OS2, EOC/LS, and EOC/MWCNT) as a function of nanofiller weight fraction (for standard deviations see Table 1).

The data presented in Table 1 and Figure 7 reveals that the addition of varied weight fraction of MWCNT and LS filler increases the hardness and indentation modulus. It can be seen that the value of L_2VH of pure EOC increases by 60% and 13% through the incorporation of 5 wt% of MWCNT and LS filler, respectively.

In contrast to MWCNT and LS filler, OS2 nanoparticles could not improve the hardness of EOC nanocomposites as revealed by the similar L_2VH values of EOC and EOC reinforced by 5% OS2 filler. Similar trends were observed in the indentation modulus of the nanocomposites compared with that of matrix polymer.

Generally, it can be stated that the dimensionality of the nanofiller geometry is mainly affecting the mechanical performance of the EOC nanocomposites such as the microindentation behavior as also shown for the tensile properties above. The dimensionality (1D, 2D, and 3D), that is, the aspect ratio, of the nanofiller is the higher reinforcing effect (if any, compare EOC/OS2), that is, 1D filler (MWCNT) > 2D filler (LS) > 3D filler (OS2).

4. Conclusions

The nanocomposites of the polyolefin-based ethylene-1-octene copolymer (EOC) and different kinds of nanofillers were successfully fabricated. Subsequently, the morphology and mechanical properties of the composites were characterized. The results can be summarized as follows.

(1) The filler of each type was dispersed in the polymer matrix quite homogeneously. The composites were not always exclusively nanocomposites as several micron-sized particles were also present. The best

compatibility between matrix and filler with respect to the filler size reduction and dispersion was observed in the composites with the LS which may be attributed to the presence of organic modifier intercalating into the layer galleries. The melting and crystallization behavior of the samples did not furnish significant difference under given experimental conditions so far.

(2) The results from tensile testing and microindentation hardness measurements demonstrate the following reinforcing ability of the fillers having different dimensionalities: 1D filler > 2D filler > 3D filler. The higher reinforcing effects of 1D and 2D fillers can be attributed to the high aspect ratio of those fillers.

(3) Depth sensitive recording indentation microhardness measurement offers a reliable and sensitive tool for the characterization of mechanical behavior of the nanocomposites.

Acknowledgments

The authors thank Mr. Werner Lebek (Institute of Physics, Martin-Luther University Halle-Wittenberg, Germany) for providing the SEM micrographs. S. Pradhan acknowledges the German Research Foundation (DFG) for supporting her research stay at Martin-Luther University Halle-Wittenberg and Nepal Academy of Science and Technology (NAST) for providing Ph. D. Research Fellowship. R. Adhikari thanks the Alexander von Humboldt (AvH) Foundation for funding his short-term stay at Martin-Luther University Halle-Wittenberg, Germany.

References

[1] M. Alexandre and P. Dubois, "Polymer-layered silicate nanocomposites: preparation, properties and uses of a new class of materials," *Materials Science and Engineering R: Reports*, vol. 28, no. 1-2, pp. 1–63, 2000.

[2] A. Biswas, A. Bandyopadhyay, N. K. Singha, and A. K. Bhowmick, "Ionomeric modification of metallocene-based polyolefinic elastomers with varied pendant chain length and its influence on physico-mechanical properties," *Journal of Materials Science*, vol. 44, no. 12, pp. 3125–3134, 2009.

[3] C. E. Powell and G. W. Beall, "Physical properties of polymer/clay nanocomposites," *Current Opinion in Solid State and Materials Science*, vol. 10, no. 2, pp. 73–80, 2006.

[4] S. S. Ray and M. Okamoto, "Polymer/layered silicate nanocomposites: a review from preparation to processing," *Progress in Polymer Science*, vol. 28, no. 11, pp. 1539–1641, 2003.

[5] R. A. Pethrick, G. E. Zaikov, and J. Pielichowski, Eds., *Monomers, Oligomers, Polymers, Composites and Nanocomposites Research: Synthesis, Properties and Applications*, Nova Science, 2009.

[6] F. Gao, Ed., *Advances in Polymer Nanocomposites: Types and Applications*, Series in Composites Science and Engineering, Woodhead Publishing, 2012.

[7] F. Ebrahimi, Ed., *Nanocomposites—New Trends and Developments*, InTech, 2012.

[8] R. Adhikari, "Atomic force microscopy of polymer/layered silicate nanocomposites (PLSNs): a brief overview," *Macromolecular Symposia*, vol. 327, no. 1, pp. 10–19, 2013.

[9] R. Adhikari and G. H. Michler, "Polymer nanocomposites characterization by microscopy," *Journal of Macromolecular Science C: Polymer Reviews*, vol. 49, no. 3, pp. 141–180, 2009.

[10] J. Tsai and C. T. Sun, "Effect of platelet dispersion on the load transfer efficiency in nanoclay composites," *Journal of Composite Materials*, vol. 38, no. 7, pp. 567–579, 2004.

[11] E. T. Thostension, L. Chunyu, and T.-W. Chou, "Nanocomposites in context," *Composites Science and Technology*, vol. 65, no. 3-4, pp. 491–516, 2005.

[12] B. J. Ash, R. W. Siegel, and L. S. Schadler, "Mechanical behavior of alumina/poly (methyl methacrylate) nanocomposites," *Macromolecules*, vol. 37, no. 4, pp. 1358–1369, 2004.

[13] J. Móczó and B. Pukánszky, "Polymer micro and nanocomposites: structure, interactions, properties," *Journal of Industrial and Engineering Chemistry*, vol. 14, no. 5, pp. 535–563, 2008.

[14] G.-M. Kim, *Verstärkungsmechanismen auf Makro-, Mikro- und Nano-Längenskalen in Heterogenen Polymerwerkstoffen*, Papierflieger, Clausthal-Zellerfeld, Germany, 2007.

[15] L. S. Schadler, L. C. Brinson, and W. G. Sawyer, "Polymer nanocomposites: a small part of the story," *Journal of Operations Management*, vol. 59, no. 3, pp. 53–60, 2007.

[16] I. M. Ward and J. Sweeney, *An Introduction to the Mechanical Properties of Solid Polymers*, John Wiley & Sons, Chichester, UK, 2004.

[17] E. P. Gianellis, "Polymer layered silicate nanocomposites," *Advanced Materials*, vol. 8, no. 1, pp. 29–35, 1996.

[18] F. J. Baltá Calleja and S. Fakirow, *Microhardness of Polymers*, Cambridge Solid State Science Series, Cambridge University Press, Cambridge, UK, 2000.

[19] F. J. Baltá Calleja, D. S. Sanditov, and V. P. Privalko, "Review: the microhardness of non-crystalline materials," *Journal of Materials Science*, vol. 37, no. 21, pp. 4507–4516, 2002.

[20] F. J. Baltá Calleja, A. Flores, and F. Ania, "Micro-indentation studies of polymers relating to nanostructure and morphology," in *Mechanical Properties of Polymers Based on Nanostructure and Morphology*, G. H. Michler and F. J. Baltá Calleja, Eds., chapter 8, p. 279, Taylor and Francis, Boca Raton, Fla, USA, 2005.

[21] W. Grellmann and S. Seidler, Eds., *Polymer Testing*, Hanser, Munich, Germany, 2007.

[22] R. Pandit, J. Giri, G. H. Michler et al., "Effect of epoxidation of diene component of SBS block copolymer on morphology and mechanical properties," *Macromolecular Symposia*, vol. 315, no. 1, pp. 152–159, 2012.

[23] T. Koch, *Morphologie und Mikrohärte von Polypropylen-Werkstoffen*, Mensch und Buch, Berlin, Germany, 2003.

[24] N. L. Bhandari, R. Lach, W. Grellmann, and R. Adhikari, "Depth-dependent indentation microhardness studies of different polymer nanocomposites," *Macromolecular Symposia*, vol. 315, no. 1, pp. 44–51, 2012.

[25] A. Flores, F. Ania, and F. J. Baltá Calleja, "From the glassy state to ordered polymer structures: A Microhardness Study," *Polymer*, vol. 50, no. 3, pp. 729–746, 2009.

[26] O. Osazuwa, K. Petrie, M. Kontopoulou, P. Xiang, Z. Ye, and A. Docoslis, "Characterization of non-covalently, non-specifically functionalized multi-wall carbon nanotubes and their melt compounded composites with an ethylene–octene copolymer," *Composites Science and Technology*, vol. 73, pp. 27–33, 2012.

[27] P. Svoboda, R. Theravalappil, S. Poongavalappil et al., "A study on electrical and thermal conductivities of ethylene-octene copolymer/expandable graphite composites," *Polymer Engineering and Science*, vol. 52, no. 6, pp. 1241–1249, 2012.

[28] G. H. Michler, *Electron Microscopy of Polymers*, Springer, Heidelberg, Germany, 2008.

[29] R. Lach, G. H. Michler, and W. Grellmann, "Microstructure and indentation behaviour of polyhedral oligomeric silsesquioxanes—modified thermoplastic polyurethane nanocomposites," *Macromolecular Materials and Engineering*, vol. 295, no. 5, pp. 484–491, 2010.

[30] ISO 14577-1, *Metallic Materials—Instrumented Indentation Test for Hardness and Materials Parameters—Part 1: Test Method*, 2002.

[31] L. E. Nielsen, "Mechanical properties of particulate-filled systems," *Journal of Composite Materials*, vol. 1, no. 1, pp. 100–119, 1967.

[32] R. Lach, G.-M. Kim, G. H. Michler, W. Grellmann, and K. Albrecht, "Indentation fracture mechanics for toughness assessment of PMMA/SiO_2 nanocomposites," *Macromolecular Materials and Engineering*, vol. 291, no. 3, pp. 263–271, 2006.